

# Lepto-Hadronic Origin of $\gamma$ -rays from the G54.1+0.3 Pulsar Wind Nebula

Hui Li<sup>1</sup>, Yang Chen<sup>1,2\*</sup> and Li Zhang<sup>3</sup>,

<sup>1</sup>*Department of Astronomy, Nanjing University, Nanjing 210093, P. R. China*

<sup>2</sup>*Key Laboratory of Modern Astronomy and Astrophysics, Nanjing University, Ministry of Education, China*

<sup>3</sup>*Department of Physics, Yunnan University, Kunming, P. R. China*

Accepted . Received ; in original form

## ABSTRACT

G54.1+0.3 is a Crab-like pulsar wind nebula (PWN) with the highest  $\gamma$ -ray to X-ray luminosity ratio among all the nebulae driven by young rotation-powered pulsars. We model the spectral evolution of the PWN and find it difficult to match the observed multi-band data with leptons alone using reasonable model parameters. In lepton-hadron hybrid model instead, TeV photons come mainly from  $\pi^0$  decay in proton-proton interaction and the observed photon spectrum can be well reproduced. The newly discovered infrared loop and molecular cloud in or closely around the PWN can work as the target for the bombardment of the PWN protons.

**Key words:** gamma rays: theory – ISM: individual (G54.1+0.3) – radiation mechanisms: non-thermal

## 1 INTRODUCTION

Pulsar wind nebulae (PWNe) are thought to be an efficient accelerator for cosmic rays with energy above the “knee”. Pulsar, located in the center of PWN, loses its energy by driving ultra-relativistic wind of electrons, positrons, and ions. However, it is hard to know the fraction of energy division of different particle components. The extended  $\gamma$ -ray emission from PWN provides an exciting opportunity for studying the acceleration and radiation mechanism of particles in ultra-relativistic shocks. It has been long debated whether the very high energy (VHE) emission from PWNe as well as from supernova remnants (SNRs) is leptonic or hadronic origin. Theoretically, it has been suggested that some fraction of the pulsar’s spin-down energy can be converted into nuclei (Cheng et al. 1990; Arons & Tavani 1994), which indicates that TeV emission from PWNe may contain contribution from both leptons and hadrons. Indeed, nucleonic models have been used to reproduce the  $\gamma$ -rays from Crab and Vela X, respectively (Atayan et al. 1996; Horns et al. 2006). Recently, the discovery of TeV emission from G54.1+0.3 by VERITAS (Acciari et al. 2010) presents a brand new case for highlighting the relative significance of hadrons in PWNe.

G54.1+0.3 is a Crab-like (Lu et al. 2002) SNR with properties very similar to the Crab Nebula in both morphology and photon spectral indices. The central pulsar,

PSR J1930+1852, has a period of  $P = 137$  ms and a period derivative of  $\dot{P} = 7.5 \times 10^{-13} \text{ s s}^{-1}$ , corresponding to a current spin-down luminosity of  $L_{sd} = 1.2 \times 10^{37} \text{ erg s}^{-1}$  and a characteristic age  $\tau_c \approx 2900 \text{ yr}$  (Camilo et al. 2002). A faint X-ray shell was most recently detected surrounding the PWN up to  $\sim 6'$  from the pulsar (Bocchino, Bandiera, & Gelfand 2009). The SNR has been suggested to be at a distance of 6.2 kpc by the HI absorption and morphological association with a molecular cloud (Leahy et al. 2008).

Recent AKARI observation discovered an infrared (IR) loop, which is explained to be a star-formation loop around the G54.1+0.3 PWN (Koo et al. 2008) and is alternatively explained to be the freshly-formed dust in the supernova ejecta (Temim et al. 2009). Using VLA radio polarization and Spitzer mid-IR observations, Lang et al. (2009) found a molecular cloud located at the southern edge of the PWN and suggested an interaction between the PWN and the cloud. In  $\gamma$ -rays, VERITAS observed the VHE TeV emission from G54.1+0.3 and found that the efficiency of converting the spin-down energy to  $\gamma$ -ray emission is high and the ratio of  $\gamma$ -ray to X-ray luminosity is as large as 0.7. This ratio, two orders of magnitudes higher than that of the Crab, is the highest among all the nebulae supposedly driven by young rotation-powered pulsars (Acciari et al. 2010). This may imply that the VHE TeV emission has extra components in addition to the contribution from commonly-acknowledged energetic leptons scattering background photons. The newly discovered IR loop and/or molecular cloud around the G54.1+0.3 PWN may act as

\* E-mail: ygchen@nju.edu.cn

an appropriate target for the energetic protons to account for high-efficiency  $\gamma$ -ray production from this unusual source (Bartko & Bednarek 2008).

In this letter, we show that the TeV emission from G54.1+0.3 cannot be accounted for by leptons alone, but can be naturally explained by introduction of a hadronic component.

## 2 MODEL AND RESULTS

### 2.1 The Pure-Lepton Case

We first try to reproduce the wide-range radiation spectrum of G54.1+0.3 from radio to TeV using a pure lepton component. For calculating the spectral evolution of the PWN, we specify the evolution of the time-dependent injection spectrum and that of the magnetic field in the following.

Let us consider the relativistic wind of leptons produced within the light cylinder of the pulsar where the spin-down power  $L(t)$  is injected into PWN. A termination shock is formed in the outflowing relativistic wind, where the ram pressure is balanced by the pressure of surrounding medium, and accelerates particles to high energies. The leptons produced inside the light cylinder of the pulsar account for the radio emission, while the wind leptons accelerated by the shock have a Fermi-type energy spectrum and contribute to the X-ray emission.

As usual, we assume that the injection spectrum of the relativistic particles  $Q_{\text{inj}}(\gamma, t)$  obeys a broken power-law

$$Q_{\text{inj}}(\gamma, t) = \begin{cases} Q_0(t)(\gamma/\gamma_b)^{-p_1} & \text{for } \gamma_{\text{min}} \leq \gamma \leq \gamma_b, \\ Q_0(t)(\gamma/\gamma_b)^{-p_2} & \text{for } \gamma_b \leq \gamma \leq \gamma_{\text{max}}, \end{cases} \quad (1)$$

where  $Q_0$  is normalization coefficient,  $\gamma$  is the Lorentz factor of the relativistic electrons and positrons, and the minimum ( $\gamma_{\text{min}}$ ), maximum ( $\gamma_{\text{max}}$ ), and break ( $\gamma_b$ ) Lorentz factors together with the energy indices ( $p_1$  and  $p_2$ ) are assumed time-independent. Parameter  $\gamma_{\text{max}}$  is obtained so as to confine the accelerated electrons within the PWN (i.e., the electrons's Larmor radius must be less than the radius of the PWN) (Venter & de Jager 2006)

$$\gamma_{\text{max}} \approx \frac{e}{2m_e c^2} \sqrt{\frac{\sigma L(t)}{(1+\sigma)c}}, \quad (2)$$

where magnetization parameter  $\sigma$  is the ratio of the electromagnetic energy flux to the lepton energy flux at the wind shock of the PWN. Parameter  $\gamma_{\text{min}} = 100$  is assumed so as to reproduce the flux of the observed minimum frequency at radio wavelengths. Bucciantini et al. (2010) found that  $\gamma_b$  is at a similar value in a narrow range of  $10^5$ – $10^6$  for several PWNe of a variety of ages, which is closely related to the working of pulsar magnetospheres, pair multiplicity, and the particle acceleration mechanisms. Therefore, here we adopt  $\gamma_b = 5 \times 10^5$  without loss of generality.

The injection spectrum can be related to the spin-down power  $L(t)$  of the pulsar at given time  $t$  by assuming that a fraction ( $\eta_e$ ) of the spin-down power is converted into lepton luminosity:  $\eta_e L(t) = \int Q(\gamma, t) \gamma m_e c^2 d\gamma$ . For a spin-down pulsar,  $L(t) = L_0 [1 + (t/\tau_0)]^{-(n+1)/(n-1)}$ , where  $L_0$  is the initial spin-down power,  $\tau_0$  the characteristic timescale, and  $n$  the breaking index (here we adopt  $n = 3$  for simplicity).

Thus the normalization parameter  $Q_0(t)$  can be derived as (Tanaka & Takahara 2010)

$$Q_0(t) = \frac{L_0 \eta_e}{m_e c^2} \left(1 + \frac{t}{\tau_0}\right)^{-2} \times \left[ \frac{\gamma_b^2 (p_1 - p_2)}{(2 - p_1)(2 - p_2)} + \frac{\gamma_b^{p_2} \gamma_{\text{max}}^{2-p_2}}{2 - p_2} - \frac{\gamma_b^{p_1} \gamma_{\text{min}}^{2-p_1}}{2 - p_1} \right]^{-1}. \quad (3)$$

On the assumption of magnetic-field energy conservation (see Tanaka & Takahara 2010 for the comparison of various approximations of magnetic field evolution),

$$\frac{4\pi}{3} R_{\text{PWN}}^3(t) \cdot \frac{B^2(t)}{8\pi} = \int_0^t \eta_B L(t') dt', \quad (4)$$

the time-varying field strength of the nebula is given by

$$B(t) = \left[ \frac{6\eta_B L_0 \tau_0 t}{R_{\text{PWN}}^3(t + \tau_0)} \right]^{1/2} \quad (5)$$

where  $\eta_B$  is the fraction of spin-down energy converted to the magnetic energy and  $R_{\text{PWN}}$  the average radius of the PWN. (In parenthesis, the magnetization parameter is thus essentially  $\sigma \sim \eta_B/\eta_e$ .) Because the young G54.1+0.3 PWN ( $\sim 2900$ yr) may be in an evolution stage before the reverse shock passage (typically at  $1 \times 10^4$ yr, e.g., Reynolds & Chevalier; Gelfand 2009), we also assume that the PWN is freely expanding at velocity  $v_{\text{PWN}}$  and thus have  $v_{\text{PWN}} \sim 550(R_{\text{PWN}}/1.8\text{pc})(t/2900\text{yr})^{-1} \text{ km s}^{-1}$ .

The volume-integrated particle number as a function of energy is described by the continuity equation in the energy space:

$$\frac{\partial}{\partial t} N(\gamma, t) + \frac{\partial}{\partial \gamma} [\dot{\gamma}(\gamma, t) N(\gamma, t)] = Q_{\text{inj}}(\gamma, t) - \frac{N(\gamma, t)}{\tau_{\text{esc}}(t)} \quad (6)$$

where  $\dot{\gamma}(\gamma, t)$  is the cooling rates of the relativistic leptons including the synchrotron radiation, the inverse Compton scattering off the cosmic microwave background (CMB) and ambient IR radiation, and the adiabatic expansion, i.e.,

$$\dot{\gamma}(\gamma, t) = \dot{\gamma}_{\text{syn}}(\gamma, t) + \dot{\gamma}_{\text{IC}}(\gamma) + \dot{\gamma}_{\text{ad}}(\gamma, t), \quad (7)$$

and  $\tau_{\text{esc}}$  is the escape timescale and can be estimated as in Bohm diffusion (e.g., Zhang et al. 2008),

$$\tau_{\text{esc}} \approx 9 \times 10^5 \left[ \frac{B(t)}{80\mu\text{G}} \right] \left( \frac{E_e}{10\text{TeV}} \right)^{-1} \left[ \frac{R_{\text{PWN}}(t)}{1.8\text{pc}} \right]^2 \text{ yr}, \quad (8)$$

where the current magnetic field strength  $80\mu\text{G}$  (see §3.1) is used. The adiabatic loss  $\dot{\gamma}_{\text{ad}} = -\gamma/t$  is the dominant cooling process for the low energy particles and insignificant for the high energy ones.

The time-dependent lepton distribution is numerically solved from the continuity equation (6). Then multi-wavelength non-thermal emission can be calculated for the process of synchrotron radiation and inverse Compton scattering, with photon spectra plotted in Figures 1 and 2 (as described below).

Here the  $\gamma$ -rays are considered to purely come from leptons scattering the soft radiation field (CMB, IR and optical photons in the Galactic plane, and the IR-optical-UV emission of possible young stellar objects (YSOs) in the IR loop). The IR background at the Galactic disc is characterized by temperature 25K and energy density two times larger than the CMB, while the optical background by temperatures between 5000 and  $10^4$  K and energy densities equal

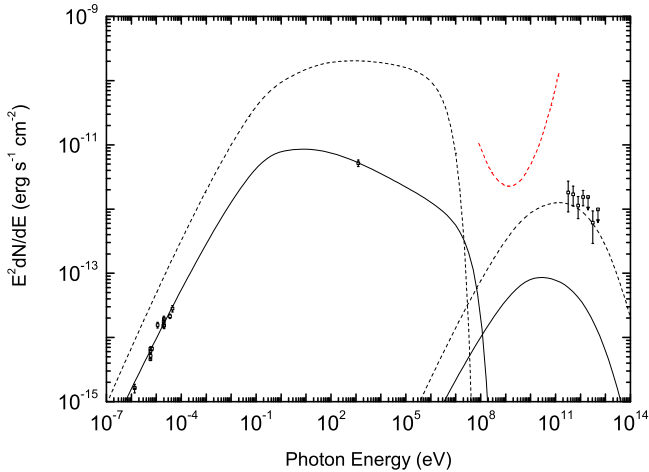


**Figure 1.** Comparison of the predicted spectra in the pure-lepton Models A (solid line) and B (dashed line) with the observed data for G54.1+0.3 in radio (Natasha et al. 2008; Lang et al. 2009), X-rays (Lang et al. 2009) and  $\gamma$ -rays (Acciari et al. 2010). The model parameters are described in the text of §2.1. The red dashed line shows the 1 year,  $5\sigma$  sensitivity for the *Fermi* LAT (*Fermi* LAT 2007).

to the CMB. The incident IR photons from the SNR are defined by a  $\sim 90$  K blackbody radiation with the energy density  $\sim 5.3 \times 10^{-12} \text{erg cm}^{-3}$  based on the Spitzer IRAC fluxes at  $24\mu\text{m}$  and  $70\mu\text{m}$  from Temim et al. (2009), a factor of roughly 5 larger than the IR energy density in the Crab Nebula and 13 larger than the energy density in the CMB. In the calculation we also take into account the possible IR-optical-UV starlight from 11 possible YSOs, which has an energy density  $\sim 4.4 \times 10^{-11} \text{erg cm}^{-3}$  with a blackbody temperature  $T \sim 35000\text{K}$  (Koo et al. 2008). The IC flux is dominated by scattering with the IR photons from the SNR, while the IC scattering with other components are insignificant by comparison. Note that the power of synchrotron self-Compton emission to synchrotron emission  $P_{\text{SSC}}/P_{\text{syn}} = U_{\text{syn}}/U_B < 10^{-2}$  (here eq.(27) in Tanaka & Takahara 2010 is used), the contribution of  $\gamma$ -ray emission for G54.1+0.3 PWN from IC scattering off the synchrotron radiation is negligible.

For the physical parameters of the PWN, we set  $L_0 \approx 1.4 \times 10^{39} \text{ergs s}^{-1}$ ,  $\gamma_b = 5 \times 10^5$ , and  $p_1 = 1.2$  according to previous studies (Camilo et al. 2002; Lang et al. 2009; Bucciantini et al. 2010) and leave other three parameters,  $\eta_e$ ,  $\eta_B$ , and  $p_2$ , adjustable. For comparison, we develop three sets of parameters for leptonic model. In Model A, we reproduce the observed results of radio to X-ray emission (which are synchrotron) and get  $\eta_e = 6\%$ ,  $\eta_B = 8\%$ , and  $p_2 = 2.4$ . As can be seen in Figure 1 (the solid line), the resulting TeV emission from leptons is lower than the observed flux by more than an order of magnitude. In Model B, we change parameters to reproduce the observed TeV emission by IC scattering soft photon fields described above. The adopted parameters are  $\eta_e = 92\%$ ,  $\eta_B = 8\%$ , and  $p_2 = 2.1$ . The resulting synchrotron radio and X-ray emission (the dashed line in Figure 1) excess the observation data by more than an order of magnitude. The current magnetic field strength for Model A

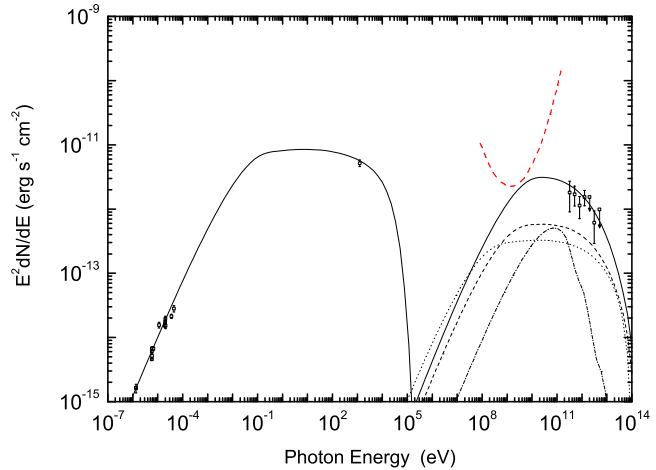


**Figure 2.** The same as Figure 1, but for pure-lepton Model C (solid line). The parameters are described in the text of §2.1. The IC flux (the solid line on the right side) is dominated by scattering with the IR photons from the SNR, while the IC scattering with the IR photons from Galactic diffusion (dashed), the CMB (dotted), and the starlight of the possible YSOs (dashed-dotted) are also shown.

and B,  $80\mu\text{G}$  (derived from observation, see §3.1), has been used in Eq.(5). In order to match both the synchrotron and IC emission to the observed data, we explore the parameter space and obtain the third model (Model C) (Figure 2) with  $\eta_e = 99.8\%$ ,  $\eta_B = 0.15\%$ , and  $p_2 = 2.8$ . However, this corresponds to a weak magnetic field  $\sim 10\mu\text{G}$ . If we adopt an age of 2000 yr for this PWN as obtained by Bocchino et al.(2009) in their dynamic evolution model, other than 2900 yr, then lower field strength would be needed in Model C. Such low values of the field strength are inconsistent with that derived from observation, as will be discussed in §3.1. Therefore, it is hard for a pure-lepton model to reproduce the radio, X-ray, and TeV data simultaneously, and thus the leptons alone cannot account for the  $\gamma$ -ray emission.

## 2.2 The Lepton-Hadron Hybrid Case

We now consider the contribution to the TeV emission from a hadronic component besides the leptonic contribution. In this model, both leptons and ions extracted from the charged polar cap region are accelerated in the rotating magnetospheres of neutron stars and PWN termination shocks (e.g., Zhang et al. 2009). For simplicity, we assume the protons gain energy from central pulsar and are represented by a power-law spectrum which is common for the acceleration process. Then the total energy of protons of the PWN is  $W_p = \int A_p E_p^{-\alpha_p} E_p dE_p = \int_0^t \eta_p L(t') dt'$ , where  $\eta_p$  is the energy fraction converted to protons,  $A_p$  the normalization coefficient and  $\alpha_p$  the spectral index of accelerated protons. So the energy released from the pulsar consists of the kinetic energy of particles ( $\eta_e$  and  $\eta_p$ ) and the magnetic energy ( $\eta_B$ ). For the energy,  $E_p$ , of the accelerated protons, the rest energy of protons ( $9.4 \times 10^8$  eV) is adopted as minimum and the energy at the “knee” ( $3 \times 10^{15}$  eV) as the maximum. Note that the energy converted into leptons and magnetic field in

Model A is only a small fraction ( $\eta_e = 5\%$  and  $\eta_B = 8\%$ , respectively) of the total spin-down energy of central pulsar. In fact, in the study of the Vela X PWN, Horns et al. (2006) have questioned where the remaining energy injected from pulsar is and suggested a hadronic origin of TeV emission. Hence, we assume  $\eta_p = 87\%$  in the lepton-hadron hybrid case (denoted as Model D).

The Bohm diffusion timescale of the PWN particles determined from Eq. (8) ( $\sim 10^4$  yr) is much longer than the PWN age. Therefore, the protons are considered to be well confined in the PWN and the escape losses of protons are negligible. The cooling time of p-p interaction is (e.g., Aharonian 2004)  $t_{pp} \approx 1.8 \times 10^6 (n_b/30 \text{ cm}^{-3})^{-1}$  yr, much longer than the age of G54.1+0.3, where  $n_b$  is the average density of target baryons in the PWN (see below). Hence the collision losses of the PWN protons are negligible as well. Also because  $t_{pp}$  is almost energy-independent in the energy region above 1 GeV, the total spectrum of protons remains unchanged (Aharonian 2004). The contribution from the secondary leptons that are created by protons interaction to the overall spectrum is negligible too, as compared with the dominant contribution of the primary leptons (Horns et al. 2006; Zhang et al. 2009).

In addition to the contribution from the leptons as given in Model A, we calculate that from p-p interaction so as to match the observed TeV flux. For the  $\pi^0$  decay ensuing from p-p collision, the analytic emissivity developed by Kelner et al. (2006) is used. It is difficult to determine the detail process of energetic protons captured by the baryonic targets, since this process depends on geometry of the PWN and the targets and anisotropy of the magnetic field and diffusion coefficient. Thus, we assume that a small fraction ( $\xi$ ) of all hadrons is captured by baryonic targets (as suggested by Bartko & Bednarek 2008). The wide-range spectrum of the PWN can now be well reproduced with  $\xi \sim 8 \times 10^{-3} (n_b/30 \text{ cm}^{-3})^{-1}$  and the results are shown in Figure 3. Here a target baryon density  $\sim 30 \text{ cm}^{-3}$  has been adopted from the estimate of the IR clump density (Temim et al. 2010); this number can also be typical of the density of the molecular materials, which Koo et al. (2009) and Lang et al. (2010) reported to detect. Apparently, even such a low capture efficiency is sufficient for hadrons to produce the observed flux of TeV emission.

### 3 DISCUSSION

In the pure-lepton case, Model C seems to marginally match the wide-range spectrum of the G54.1+0.3 PWN; by comparison, however, the lepton-hadron hybrid case (Model D) can reproduce the spectrum better and more physical in the following aspects.

#### 3.1 Magnetic field

In §2.1, the field strength obtained in Model C (the lepton case) is  $10 \mu\text{G}$  or even lower. Such values of field strength are actually weaker than that derived from observation. Based on radio luminosity, Lang et al. (2009) derived an equipartition field of  $38 \mu\text{G}$ . However, they suggested stronger field in the light of the strong polarization which is organized on large scales of the nebula and implies the PWN is filled

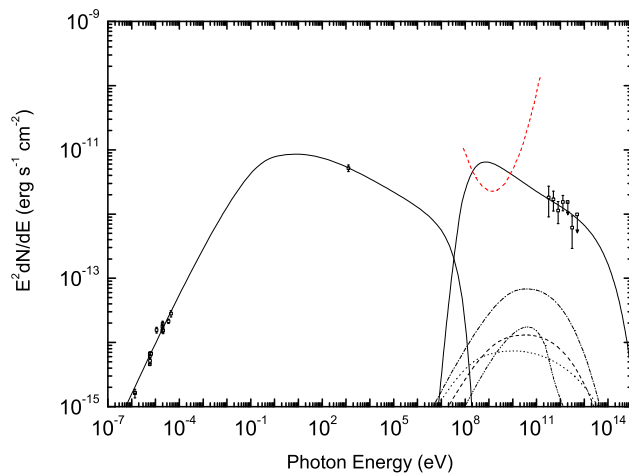


**Figure 3.** The same as Fig.1, but for lepton-hadron hybrid Model D. The parameters are described in the test of §2.2. The solid line on the right side is dominated by  $\pi^0$  decay ensuing from p-p interaction. The inverse Compton scattering with IR photos from SNR (dashed-dotted line), IR photos from Galactic diffusion (dashed), starlight of the possible YSOs (dashed-dotted-dotted) and the CMB (dotted) are also shown.

with magnetically-dominated plasma. They also found an alternative field strength of  $80\text{--}200 \mu\text{G}$  by using the lifetime of the X-ray emitting particles. In Model D (the lepton-hadron case), however, we use  $80 \mu\text{G}$  which can typify the field strength estimated by Lang et al.

#### 3.2 TeV index

In Model C, the calculated TeV slope ( $\sim 2.6\text{--}3$ ) of the IC spectrum cannot well match the VERITAS data point (with photon index 2.4, Acciari et al. 2010). Matching the TeV slope would entail a lepton ensemble with a unreasonable large energy index 3.8. Even if the energy losses in high energy leptons are considered, we, using the time-dependent model, find the energy index of accelerated leptons by relativistic shock is 2.8, still considerably higher than the universal power-law index 2.2–2.3 for Fermi-type acceleration by the shock of large Lorentz factor using different approaches (e.g., Horns et al. 2007). As a contrast, the observed slope is easily reproduced by protons p-p interaction with a mild proton index  $\alpha_p = 2.4$ . This proton index is fortuitously similar to the lepton index that is used to reproduce the synchrotron X-rays in Model A.

#### 3.3 Baryonic targets

The IR loop closely around the G54.1+0.3 PWN discovered by AKARI was suggested to be star-forming region (Koo et al. 2008), while it was also argued to be the freshly formed supernova dust heated by early-type stars belonging to a cluster in which the supernova exploded (Temim et al. 2009). It was also reported that a molecular cloud is found to be located at the southern edge of the PWN by the VLA radio

and Spitzer mid-IR observations and thus an interaction between the PWN with the cloud was suggested (Lang et al. 2009). These components within or surrounding the PWN, whatever they are, may readily be a baryonic target for the bombardment of the PWN protons, and therefore it is very reasonable to expect the  $\gamma$ -ray contribution from the hadron interaction. This is the very case that we address in Model D. This scenario seems to naturally explain the exceptionally high  $\gamma$ -ray to X-ray luminosity ratio of G54.1+0.3 among all the rotation-powered PWNe.

The *Fermi* observation at GeV band will be important to discriminate between the leptonic model and the hadronic model. In the pure-lepton model (cases A, B, and C; see Figures 1 and 2), the theoretical GeV  $\gamma$ -ray flux of the PWN is basically below the 1 year,  $5\sigma$  sensitivity of the *Fermi* LAT, while the lepton-hadron hybrid model (case D; see Figure 3) predicts a GeV flux above the sensitivity.

#### 4 CONCLUSION

We have calculated the multi-band non-thermal emission from the G54.1+0.3 PWN in both the pure-lepton case and the lepton-hadron hybrid case. In the lepton case, we find that the leptons that are responsible for the radio and X-ray synchrotron cannot alone account for the TeV  $\gamma$ -ray emission by IC scattering. An addition of hadron contribution by p-p interaction can well reproduce the observation spectrum. The lepton-hadron hybrid scenario is strongly supported by the most recently discovered IR loop and molecular cloud in or closely around the PWN. This scenario can also shed light on the study of the PWNe with high  $\gamma$ -ray to X-ray luminosity ratios.

#### ACKNOWLEDGMENTS

We thank Q. Daniel Wang, Rino Bandiera, and the anonymous referee for helpful comments on the manuscripts. Y.C. acknowledges support from NSFC grant 10725312. L.Z. acknowledges support from NSFC grants 10778702 and 10803005 and Yunnan Province under grant 2009 OC. The authors also acknowledge support from the 973 Program grant 2009CB824800.

#### REFERENCES

Acciari, V. A., et al. 2010, arXiv:1005.0032  
 Aharonian, F. A. 2004, Very high energy cosmic gamma radiation : a crucial window on the extreme Universe, by F.A. Aharonian. River Edge, NJ: World Scientific Publishing, 2004,  
 Arons, J., & Tavani, M. 1994, ApJS, 90, 797  
 Atoyan, A. M., & Aharonian, F. A. 1996, MNRAS, 278, 525  
 Bartko, H., & Bednarek, W. 2008, MNRAS, 385, 1105  
 Bocchino, F., Bandiera, R., & Gelfand, J. 2010, arXiv:1004.3515  
 Bucciantini, N., Arons, J., & Amato, E. 2010, arXiv:1005.1831

Camilo, F., Lorimer, D. R., Bhat, N. D. R., Gotthelf, E. V., Halpern, J. P., Wang, Q. D., Lu, F. J., & Mirabal, N. 2002, ApJL, 574, L71  
 Cheng, K. S., Cheung, T., Lau, M. M., Yu, K. N., & Kwok, P. W. 1990, Journal of Physics G Nuclear Physics, 16, 1115  
*Fermi* LAT Performance 2007, [http://www-glast.slac.stanford.edu/software/IS/glast\\_lat\\_performance.htm](http://www-glast.slac.stanford.edu/software/IS/glast_lat_performance.htm)  
 Gelfand, J. D., Slane, P. O., & Zhang, W. 2009, ApJ, 703, 2051  
 Horns, D., Aharonian, F., Santangelo, A., Hoffmann, A. I. D., & Masterson, C. 2006, A&Ap, 451, L51  
 Horns, D., Aharonian, F., Hoffmann, A. I. D., & Santangelo, A. 2007, Ap&SS, 309, 189  
 Hurley-Walker, N., et al. 2009, MNRAS, 396, 365  
 Kelner, S. R., Aharonian, F. A., & Bugayov, V. V. 2006, PRvd, 74, 034018  
 Koo, B.-C., et al. 2008, ApJL, 673, L147  
 Lang, C. C., Wang, Q. D., Lu, F., & Clubb, K. I. 2010, ApJ, 709, 1125  
 Leahy, D. A., Tian, W., & Wang, Q. D. 2008, AJ, 136, 1477  
 Lu, F. J., Wang, Q. D., Aschenbach, B., Durouchoux, P., & Song, L. M. 2002, ApJL, 568, L49  
 Reynolds, S. P., & Chevalier, R. A. 1984, ApJ, 278, 630  
 Tanaka, S. J., & Takahara, F. 2010, ApJ, 715, 1248  
 Temim, T., Slane, P., Reynolds, S. P., Raymond, J. C., & Borkowski, K. J. 2010, ApJ, 710, 309  
 Venter, C., & de Jager, O. C. 2006, in Proc. 363rd WE-Heraeus Seminar on Neutron stars and pulsars, ed. W. Becker & H.-H. Huang (MPE Rep. 291) (Garching: MPI extraterr. Phys.), 40  
 Zhang, L., Chen, S. B., & Fang, J. 2008, ApJ, 676, 1210  
 Zhang, L., & Yang, X. C. 2009, ApJL, 699, L153

This paper has been typeset from a  $\text{\TeX}$ / $\text{\LaTeX}$  file prepared by the author.